BULLETIN OF THE POLISH ACADEMY OF SCIENCES
TECHNICAL SCIENCES, Vol. 58, No. 2, 2010
DOI: 10.2478/v10175-010-0026-2

Mechanisms for self-assembling topography formation in low-temperature vacuum deposition of inorganic coatings on polymer surfaces

J.M. LACKNER[1]*, W. WALDHAUSER[1], A. ALAMANOU[1], C. TEICHERT[2], F. SCHMIED[2], L. MAJOR[3], and B. MAJOR[3]

[1] Joanneum Research Forschungsges.M.B.H., Laser Center Leoben, Leobner Strasse 94, A-8712 Niklasdorf, Austria
[2] Institute of Physics, University of Leoben, Franz-Josef Strasse 12, A-8700 Leoben, Austria
[3] Institute of Metallurgy and Materials Science, 25 Reymonta St., 30-059 Cracow, Poland

Abstract. Functionalization of surfaces is an important task for nanotechnology to add specially designed physico-chemical properties to materials. Besides chemical modification of surfaces, physical adaptations gain increasing interest. Thus, understanding the influences of film deposition on surface topography formation is the basis for future developments. For physical or chemical vapour deposited (PVD, CVD) films, structure zone models were developed, clearly showing the influences of temperature and vapour energy and, thus, surface and bulk diffusion on film structures based on four different structure zones. Generally, similar zones are also found in PVD coatings on polymeric substrates; However, due to restrictions in coating temperatures due to the thermal resistance of most polymers, the coating temperature is restricted to mostly 50°C, excluding thermal activation of at least surface diffusion of inorganic materials (metals and their nitrides, oxides, carbides, etc.) and resulting in columnar growth with dome-shaped column tops. Additionally, the high difference in mechanical properties between "stiff" inorganic coatings and "flexible" polymers implicates stress-induced growth phenomena, resulting in wrinkling, cracking and finally the formation of a superseding structure, depending on substrate and film materials and the vapour energy of the deposition method.

Key words: topography, roughness, coatings, pulsed laser deposition, magnetron sputtering, polymers.

1. Introduction

The topography of surfaces is an important property for the contact of a component to its surrounding. The tribological behaviour, the decorative appearance and even the interaction to biological matter (cells, bacteria, and tissue) is strongly influenced by the texture in macro-, micro- and nano-scale. Shape deviations, waviness, grooves, etc. are some of the macro- and micro-scaled topography features, while nano-scale features include the roughness due to the microstructure and due to the atomic arrangement (lattice). It's quite clear, that mainly the nano-scale features gain more and more interest for functional surfaces in sensors, electronics, medical and implant technology and mechanical engineering.

Nanostructures between atomic and micrometer size (generally between 1–100 nm) can be achieved by a multitude of techniques, developed since the early 1990s. Two totally different approaches are used both in laboratory and in industrial scale to generate nanostructured surfaces: The "top-down" processes structure a microscopic system by miniaturized macroscopic techniques, which technologically limits their application. Examples for such processes are ion-beam milling, laser ablation and nano-embossing. "Bottom-up" processes are based on system of nearly thermodynamical equilibrium, forming statistically-distributed to high-ordered self-organizing nanostructures. Such systems are often found for polymer surfaces, but also for inorganic and organic thin materials. They are of great interest due to their easier and faster manufacturing in larger sizes and quantities. Vacuum coating techniques, like the processes of physical and chemical vapour deposition (PVD and CVD) result generally in such statistically-distributed structures with nanotopography.

PVD covers a broad class of vacuum coating processes in which material is physically removed from a source by evaporation or sputtering, transported through a vacuum or partial vacuum by the energy of the vapour particles, and condensed as a film on the surfaces of appropriately placed parts or substrates [1]. Chemical compounds are deposited by either using a similar source material, or by introducing a reactive gas (nitrogen, oxygen, or simple hydrocarbons) containing the desired reactants, which react with metal(s) from the PVD source. In contrast, thermally or plasma activated chemical reactions in the gas phase trigger the deposition of coatings on the substrate surface in CVD. PVD processes can be classified by the technique of vaporization: Evaporation techniques require the input of thermal energy to the target material by thermal heating, electron beams, laser beams or arcs for its vaporization / sublimation. Sputtering is based on "atomizing" the target by impinging gas ions, accelerated by magnetic fields ("magnetron sputtering") and (pulsed) direct current (DC) to radio frequency power. Ionization and plasma formation is found in all the higher energetic techniques (thus, all mentioned except thermal evaporation). Ion assistance by additional ion sources is partly used to increase the energy in the vapour.

*e-mail: Juergen.Lackner@Joanneum.at

Two examples for processes of very different vapour (plasma) energy are magnetron sputtering and pulsed laser deposition (PLD). In PLD, a pulsed laser is focussed onto the target to locally ablate atoms during the nano- to femtosecond long pulses. Interaction of the laser beam with the formed vapour triggers the ionization of a huge particle fraction (40–60%) [2, 3]. In sputtering, a negative voltage of typically -300 V and more attracts positive ions to the target surface at speed. The magnetic field in magnetron sputtering traps secondary electrons close to the targets, which follow helical paths around the magnetic field lines and undergo more ionizing collisions with neutral gas species than for normal sputtering [1].

Deposition of coatings on polymer materials implicates serious problems in many vacuum coating processes due to the specific conditions: Generally, the evaporation or sputtering of the target material as well as the condensation on the substrate results in heating and elusive chemical compounds (like water or diluents) in the chemical composition of the polymer disturb evacuation ("outgassing"). Additionally, the very different properties of the deposited inorganic species and the organic polymer substrate result in decisive changes in film formation compared to metal or ceramic substrates [4]: Polymers (without fibre fillers) are soft (low Young's modulus, low hardness, high yield strain, low yield stress, visco-elastic behaviour) and have high thermal expansion coefficients. Additionally, their stability for short-wavelength radiation (UV, X-ray, etc.) as well as their chemical stability is often low. Furthermore, a lot of polymers are highly reactive due to their organic, macromolecular chemical composition containing C, H, O, N, Cl etc. atoms.

Nevertheless, this drastically different behavior between the substrate and the film leads to interesting film growth phenomena, resulting in the formation of micro- to nanometer scaled topographical features [4] in self-assembling surface structures. The current work will show and explain the origins of and influences on these film growth phenomena on organic polymer substrates including the well scientifically accepted inorganic film growth theories for metal and ceramic substrates and mechanics theories of compound deformation. Due to the thermal sensitivity of polymers, we will focus on low temperature (room temperature) coating techniques, overviewing both low- and high-energetic film formation conditions in magnetron sputtering, PLD and ion source based PACVD (plasma activated chemical vapour deposition), respectively.

2. Fundamental influences to thin film formation

The nucleation and growth of thin film in vacuum deposition processes is based on the condensation of vaporized species on a solid substrate surface. Forming chemical bonds to the surface atoms of the substrate (nucleation) or the growing film as well as the proper geometrical alignment for crystallization are the most important processes during deposition. They are highly dependent on the binding energy for adsorption/desorption of the film atoms (molecules) as well as on the possibility of the deposited species for diffusion on or subjacent to the new formed surface.

2.1. Vapour energy in vacuum deposition. To trigger adsorption/desorption and diffusion processes (see below), it's necessary to at least provide the energy for their activation, which is generally thermal vibration energy. Besides of heating the substrate energy input is also possible by energetic deposited species (ions or accelerated atoms – ionic or kinetic energy) [5, 6]. Generally an energy transfer occurs, when a positive ion or accelerated atom collides with atoms at the surface of a solid. This results in various processes – see Fig. 1. While species of thermal energy are only able to physisorb or chemisorb on the existing surface and do not disturb surface or subjacent atoms [7], hyperthermal species (>10 eV) can abstract atoms from surfaces (abstraction reactions) or dissociate and scatter other species, if they are polyatomic (dissociative scattering). The ions also may react with the substrate atoms to create altogether new chemical species. These new chemical species may be volatile or readily sputtered, leading to surface etching (reactive ion etching). The ions may directly react with the surface atoms to form new species (e.g., oxide/nitride growth).The energy input in the surface can induce secondary collisions of substrate atoms which cause collision cascades and result in energy transfer far from the initial impact point. The effects of the impacting ion migrate further into the bulk region of the substrate and away from the impact point with increasing ion energy. Higher energy input (>100 eV) causes sputtering of surface atoms as ions or neutrals (ion sputtering), annealing of the surface, mixing of surface atoms, creation of unique surface topologies, and defect formation. As the ion energy increases into the highest energy range known for coating processes (1000–10000 eV), the ion–surface interaction moves from predominantly nuclear – nuclear collisions between projectile and target to one that is primarily electronic in nature [8]. These low energy ions can easily implant into the surface to form an alloy or doped material (ion implantation).

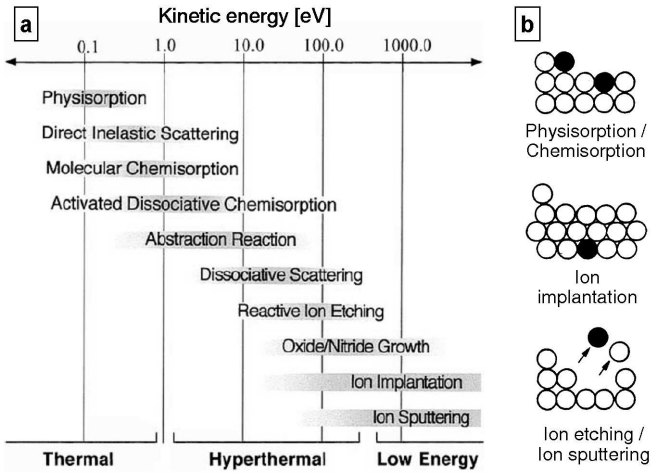

Fig. 1. a) Fundamental processes occurring in the interaction between vaporized (ionised) atoms/molecules and the solid surfaces. The shaded region designates the ion kinetic energy range over which the associated process is evident; b) The schematics present simplified the most important processes of this interaction (adapted from Refs. 1, 7, 9)

If the energy transferred to a lattice site is greater than the binding energy, primary recoil atoms can be created which can collide with other atoms and distribute their energy via collision cascades. A surface atom becomes sputtered if the energy transferred to it normal to the surface is larger than about 3 times the surface binding energy (approximately equal to the heat of sublimation).

The energy distribution in the vaporized particle flux is very dependent on the method of vaporization: In PLD, generally two particle fractions are evident [3] – the high-energetic fraction with ion energies between 100 and 1000 eV at the plasma expansion front and the low-energetic with 10 to 50 eV ions or accelerated atoms. The latter contains about 30–70% of the ablated material close to the ablation area. In magnetron sputtering, the energy of the vaporized particles is generally below 30 eV with a degree of ionization $<$1–5% [1]. Pulsing a DC magnetron plasma in the kHz range slightly increases the vapour energy. In ion and plasma sources, the ion or plasma energy is a function of the ion acceleration voltage and can be varied up to several keV.

Particles (ions or accelerated atoms) would reach the substrate surface with this energy at "molecular flow" conditions, describing the high-vacuum case, in which the mean free path of gas molecules is longer or equal to the target substrate distance (generally $\sim$10–15 cm far from the target) [10]. This corresponds to process gas pressures of $\sim$0.001 mbar or lower, depending on the gas species. Scattering of the vaporized species with the background (process) gas occurs at higher pressures in the "viscous flow" (fluid flow) regime, where gas flows as a fluid and the mean free path is much smaller than the target-substrate distance. PLD and magnetron sputtering work in both the molecular and viscous flow regimes and, thus, open a wide process window in deposition [10]. During scattering, particle energy is transferred to the process gas and not available to activate processes requiring high energetic as described above. Energy loss follows an exponential decrease with increasing number of hits [Lackner, unpublished results] and scattering results in a deviation of the particle from its straight movement towards the substrate. However, species with higher energy after evaporation/sputtering would commonly reach the substrate surface with higher energy.

2.2. Growth kinetics in thin films – structure zone models. During continuous film formation after the nucleation, the structure is generally dependent on the four basic processes, which are involved in the atomic odyssey between arrival on the substrate surface and integration in the growing film [11]. These mechanisms are shadowing, surface diffusion, bulk diffusion, and desorption. The last three are quantified by diffusion and sublimation activation energies, whose magnitudes scale directly with the melting point of the film. Shadowing is a phenomenon arising from the geometric constraint imposed by the roughness of the growing film and the line-of-sight impingement of arriving atoms.

Introducing the "homologous" or "reduced" temperature – the ratio of the substrate temperature (T_s) to the melting point of the film (T_m), T_s/T_m – allows a general description of the evolving structural morphologies in three structural zones (Zone 1, 2, 3) [12] in structure zone models (SZM, Fig. 2a). Additionally to the temperature influence, structures also changes with the amount of additional energy, being delivered to the growth surface, resulting in a fourth "transitional" zone (Zone T) between Zone 1 and 2 for energy-enhanced processes [5].

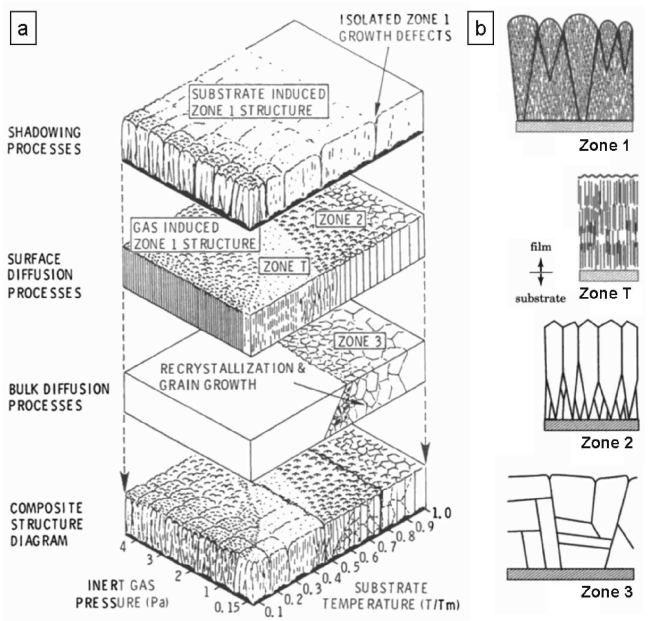

Fig. 2. a) schematic representation showing the superposition of physical processes which establish structural zones, Ref. 13 – (taken from Ref. 14); b) Characteristics of the four basic structural zones in cross section (taken from Ref. 10)

The formation and microstructure of the structural zones can be described as following (Fig. 2b):

– Zones of quenched growth – negligible (temperature activated) surface diffusion. The diffusion length is smaller than the next-neighbours distance ($\Lambda < a$)[1]:

[1]Surface diffusion can generally be thought of in terms of particles jumping between adjacent adsorption sites on a surface and is thermally promoted with rates increasing with increasing temperature. The attempt frequency ν influencing the jump rate (Γ) on a 2D surface lattice between nearest-neighbour adsorption sites (a) is typically taken to be simply the vibration frequency of the adatom. Thermodynamics in diffusion includes both the temperature and the potential energy barrier. This energy barrier to diffusion must be smaller than the energy of desorption, otherwise desorption processes would dominate. The diffusion length ? of an atom or molecule in time t can be approximated based on random walk statistics. Introducing the temperature dependent surface diffusion rate (D) results in the approximation (Eq. 1):

$$s^2\langle\Delta^2\rangle = a^2\Gamma t = 4Dt \sim \Lambda \tag{1}$$

Surface diffusion rates and mechanisms are affected by a variety of factors including the strength of the surface-adatom bond, orientation of the surface lattice, attraction and repulsion between surface species and chemical potential gradients.

- Zone 1 consists of columns typically tens of nm in diameter separated by voids a few nm across. The columns have poor crystallinity (many defects) or are amorphous. In thicker films they become superimposed upon this structure an array of cones with wider voids between them. The cones terminate in domes at the surface and the size of the domes increase with film thickness.
- Zone T occurs generally in energy-enhanced processes and collision-activated surface diffusion. It contains defected columns similar to those of Zone 1, but the voids and domes are absent.

– Zones of thermally activated growth and, at least, activated surface diffusion. The diffusion length is larger than the next-neighbours distance ($\Lambda > a$):

- Zone 2 occurs at $T_s/T_m > 0.3$, which is high enough for activating surface diffusion. It consists of columns having tight grain boundaries between them and having a characteristic diameter which increases with T_s/T_m. Crystalline columns are less defected than in Zone 1 and T and are often facetted at the surface.
- A transition to Zone 3 occurs at $T_s/T_m > 0.5$, which is high enough for activating bulk diffusion in the film. The film is annealed just during deposition, resulting in more isotropic, equiaxed crystallite shapes. Film surfaces are often smooth, but grain boundaries can develop grooves.

3. Experiments

3.1. Thin film deposition. The deposition of the coatings was performed on PVD coating equipment at Laser Center Leoben (detailed description see [4, 15]). For simulating various energetic conditions during deposition, we used (with increasing medium vapour energy) DC and pulsed DC magnetron sputtering (balanced, unbalanced), PLD and ion-source based PACVD (average energy ranges of the different techniques see above, PACVD: highest particle density with $\sim$750 eV).

Before deposition, we cleaned the substrates (polyamide (PA), polycarbonate (PC), polyimide (PI), polyurethane (PU)) ultrasonically with ethanol. Table 1 gives an overview of the most important properties for coating of these polymers. After mounting the substrate in parallel to the target surface in $\sim$120 mm distance, we pumped the vacuum chamber down to at least 4×10^{-5} mbar. Titanium as well as gold films were deposited by PLD (Nd:YAG laser, 1064 nm wavelength, 10 resp. 50 Hz pulsing, 10 ns pulse length) from pure Ti (>99% purity) and Au (999) targets in argon atmosphere. To simulate different energetic conditions during PLD deposition of titanium, we applied different argon gas pressures for scattering of the ablated vapour ("Ti – high p" for low and "Ti – low p" for high energetic deposition), covering the transition between molecular and viscous flow regimes. Furthermore, Ti was also deposited by balanced DC magnetron sputtering. Titanium nitride (TiN) was reactively deposited by both PLD and unbalanced DC magnetron sputtering in argon-nitrogen atmospheres from Ti targets. Diamond-like carbon (DLC) films were grown with low hydrogen contents ($\sim$13 at.%, a-C ([16] for H contents)) by pulsed DC, balanced magnetron sputtering (80 kHz frequency) in inert Ar process gas from carbon targets, with higher H content and Ti-doping ($\sim$28 at.%, a-C:H:Ti) from titanium targets in C_2H_2 atmosphere and with $\sim$22 at.% H with anode layer ion source (ALS) based PACVD in C_2H_2 atmosphere and, differently from all other techniques (except PLD under low pressure), in the molecular flow regime. Growth of all coatings in different thicknesses from 5 nm to 2 μm was achieved between room temperature and 50°C.

Table 1
Most important properties of PC, PI, PA and PU for vacuum coating [17]

	PC	PI (pseudo-thermoplastic)	PA 6.6	PU (thermoplastic, TPE-U, TPU)
Density [g/cm^3]	1.2	1.27	1.12–1.15	1.10–1.25
Yield strength [MPa]	>55		60–65	
Elongation at yield [%]	6		17	
Tensile strength [MPa]	>65	75–90	70–90	52
Elongation at fracture [%]	>100	4–8	170	500
"Elastic modulus" (tension), 23°C [MPa]	2300	3200	2700–3000	50–500
Vicat softening temperature VST/B [°C]	145–150	219		
Melting temperature [°C]	267	None	255–265	60–80
Thermal expansion coefficient [10^{-5} K^{-1}]	7	5.5	7–10	
Thermal conductivity [W/mK]	0.21	0.52	0.27	
Water absorption at 23°C/saturation [%]	0.35	1.25	8.5	
Microstructure	Macromolecular chains with no crosslinking			Macromolecular chains and crystalline, crosslinking segments (20–30 nm diameter)

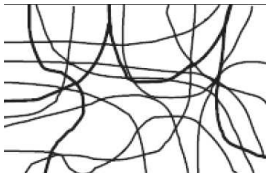

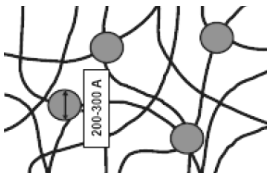

3.2. Characterization. The microstructure of the coatings was investigated using high-resolution transmission electron microscopy (TEM, TECNAI G2 F20-TWIN (200 kV)). The surface topography images was observed using scanning electron microscopy (SEM, 20 kV), atomic force microscopy (AFM) in the tapping mode (DI, Dimension 3100/Asylum Research MFP 3D) and Olympus AC 160 TS silicon tips (tip radius <15 nm). The analysis of the acquired data was done using different software packets ("TrueMap" [18], WSxM [19], Gwyddion [20]) in order to obtain both amplitude parameters (geometrical/root mean square roughness, RMS) to describe the height differences and lateral frequency parameters (average 1^{st} neighbour distance, lateral correlation length [21]. While the roughness parameters and their calculation are generally known, lateral frequency parameters are scarcely used yet to describe the surface topography, although a lot of physicochemical phenomena on the surface are strongly influence by e.g. number of peaks per area, the lateral correlation length or the jaggedness of a surface. For a random rough surface with a cut-off, the lateral frequency of roughness is described by the lateral correlation length which is a measure for the lateral distance across which height of the surface are correlated [22]. Generally, it corresponds to the minimum lateral feature size and is smaller than the average feature size [23]. For analysing the growth of PVD films on polymers, spatial filtering was applied for the polymers surfaces in order to remove scratches and other huge substrate surface deviations from the analysis and plots.

4. Results and discussion

Soon after exposure of a substrate to the incident vapour in PVD and CVD coating, a uniform distribution of small clusters or islands is generally observed. The mobility of these nuclei is dependent on the possibility of surface diffusion and, thus, the substrate temperature. If the temperature is too low and the bonding of the arriving vapour to the surface is high enough, surface diffusion cannot be activated sufficiently and the atoms become immobilized where they land ("quenched growth") [11]. Finally, the whole surface is covered in both cases – however, the density of covering is different: While the possibility of surface diffusion allows the nuclei to grow in size due to binding of nearby deposited atoms and minimizing the number of gaps (voids) between the nuclei, the lack of surface diffusion leads to voids of sub-atom size between the immobilized atoms. Consequently, the surface topography is very different: If nuclei are forming, surface is at some monolayer thickness either covered by island-like nanocrystals (Volmer-Weber growth) or homogenously covered by dense single layers on top of single layers (layer-by-layer growth mode, Frank-van-der-Merwe growth), if covering the substrate by atoms increases or decreases the surface energy, respectively [24, 25]. Furthermore, a mixture of both growth modes is possible, known as layer-plus-island growth (Stranski-Krastanov growth). In the case of quenched growth, the topography forms due to statistical roughening (statistical fluctuation in the vapour arrival flux) followed by self-shadowing (angular distribution in the vapour flux) [11].

In coating of polymers with PVD techniques (e.g. PLD), we found in detailed studies of binding and mixing at the interface between the polymer and the inorganic coating the incorporation of metal atoms in the polymer chains – and, thus, very high bond strength [26]. Restrictions of the substrate temperature to <50°C due to the low thermal properties of most polymers (low glass transition or melting temperature) prevents any thermal activation of surface diffusion of inorganic coating materials (metals, ceramics), generally melting at >600°C (aluminium) to several thousand °C. So, quenched growth is one of the basic mechanisms of vacuum coating growth on polymers, if they are not sufficiently energized (ions, accelerated atoms of hyperthermal energy (>10 eV)) during sputtering/evaporation/ablation at the target.

Comparing the AFM images of uncoated and very thin (5 nm) titanium coated polymer surfaces, changes in the structures are well visible for both PC (Fig. 3a,b) and PU (Fig. 3c,d) substrates. Both substrates are flat and smooth on the nanometer scale (see detailed 2d and 3d views), but not on the micrometer scale. The dots evident in the detail of PU are due to the crystalline segments, as shown in schematic microstructures in Table 1. When ∼5 nm coatings are deposited, small islands-like structures of Ti (or Ti mixed with oxygen and carbon) [23] are developing, which are about 10–15 nm high and have a diameter <15–20 nm on PC. On PU, their height is 5 nm and their lateral distance (or diameter) is <50 nm – however, these structures on PU seem to be better interconnected than on PC. The topography of 5 nm thick Ti films on PI is quite similar to PC with slightly higher interconnection. Similar results were found for the Au layers on PC and PI. Based on the nucleation theories [24, 25], the size of these islands on all the investigated substrate-coating combinations is much larger than being expected for a Volmer-Weber island growth at the low temperatures (missing temperature activated surface diffusion) and the PLD deposition at higher pressure (lower particle energy due to more scattering at the more fluid flow-like conditions). For example island sizes of 5 nm diameter and 1–2 nm height and, thus, real Volmer-Weber growth were found for ∼5 nm thick Ti and ZrO_2 PLD films on silicon substrates [4]. Thus, we think that the growth appears under quenched growth conditions and the formation of the island-like topography has different origins.

Our opinion is supported by the TEM investigation of different 50 nm thick films on PU: Figs. 4a,c and d reveal a full, homogenous covering of the surface, following a curved substrate topography, which is in the same dimension than the topography features of 50 nm thick films (compare e.g. Fig. 7b with a 20 nm thick film). Layers of sputtered amorphous-like titanium-doped DLC (Fig. 4a,b), sputtered (Fig. 4c) and PLD nanocrystalline Ti (Fig. 4d) are formed on the amorphous-like polyurethane. Visible voids (down to the nm size) in the microstructure are missing (see detail of Fig. 4a in 4b), which seems to be due to the multidirectional incidence and even in magnetron sputtering low kinetic or ion activation of the vaporized particles on the substrate surface (see the explana-

tions below). This energetic activation in growth even in the low energetic sputtering method is visible along the interface Fig. 4b: Binding of the coating on the polymer surface occurs in a mixed (DLC + PU) interface of 1–3 nm thickness, resulting from slight implantation of deposited carbon atoms into the PU surface. Similar, but much more pronounced effects were found by the authors for higher energetic deposition of Ti with PLD on PU elsewhere [26]. All these results are distinct hints for homogenous, full covering of the surface even at a few nanometer film thickness.

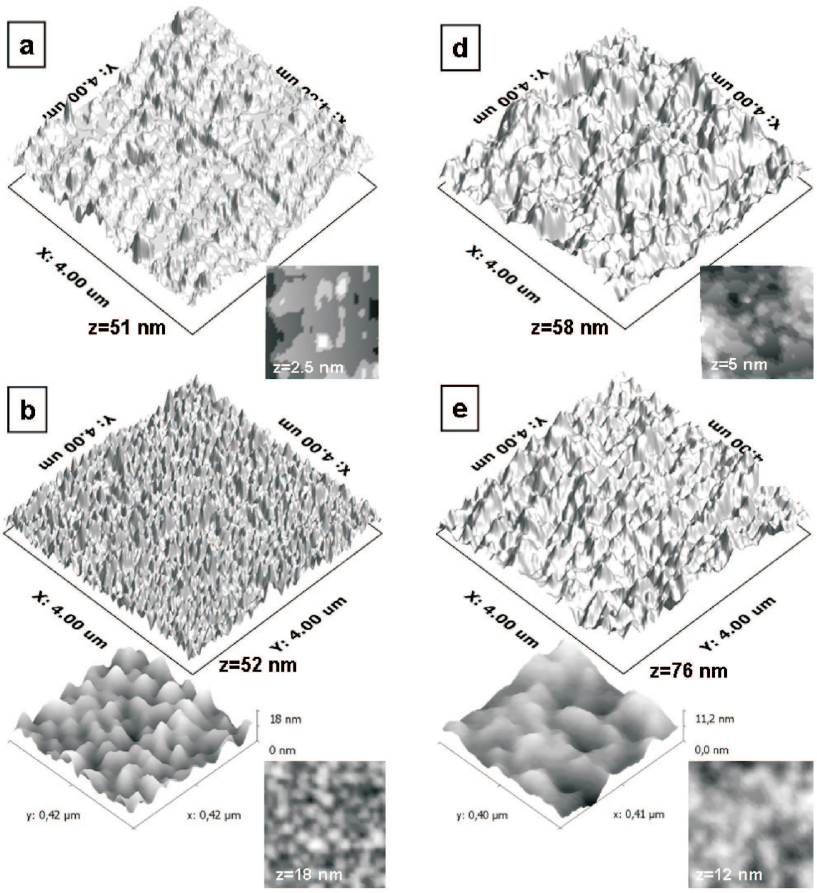

Fig. 3. Three-dimensional AFM images of nucleation and growth structures of 5 nm thick PLD Ti coatings on b) PC and d) PU surfaces, which are shown uncoated in a) and c), respectively. The details of $\sim 400 \times 400$ nm^2 large areas show the nanostructure in two- and three-dimensional views

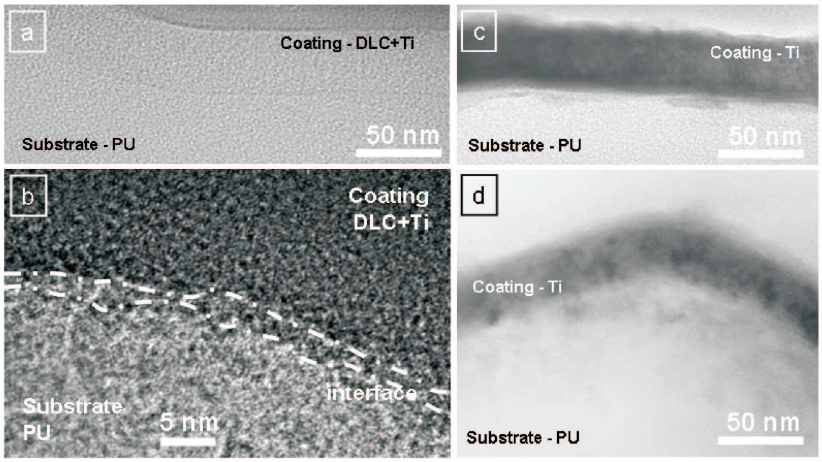

Fig. 4. TEM images of nucleation and growth structures close to the interface of 50 nm thick PVD coatings on polyurethane (PU): a), b) Magnetron sputtered titanium-doped diamond-like carbon (DLC, a-C:H:Ti) (b: magnified detail of a)), c) magnetron sputtered Ti, and d) PLD Ti

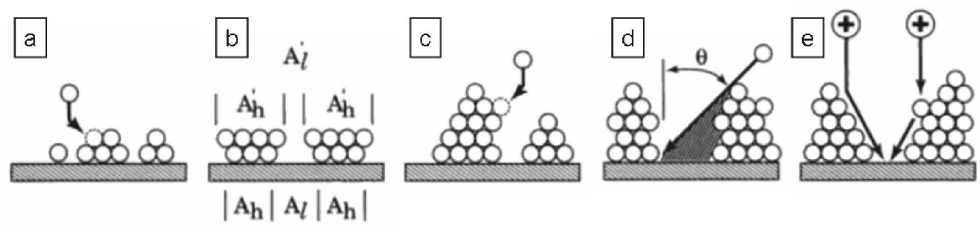

Fig. 5. Atomistic processes in quenched-growth structure development: (a) ballistic aggregation, (b) finite-size effect, (c) sideways attraction, (d) oblique shadowing, (e) void-filling by energetic particles (adapted from Ref. 11)

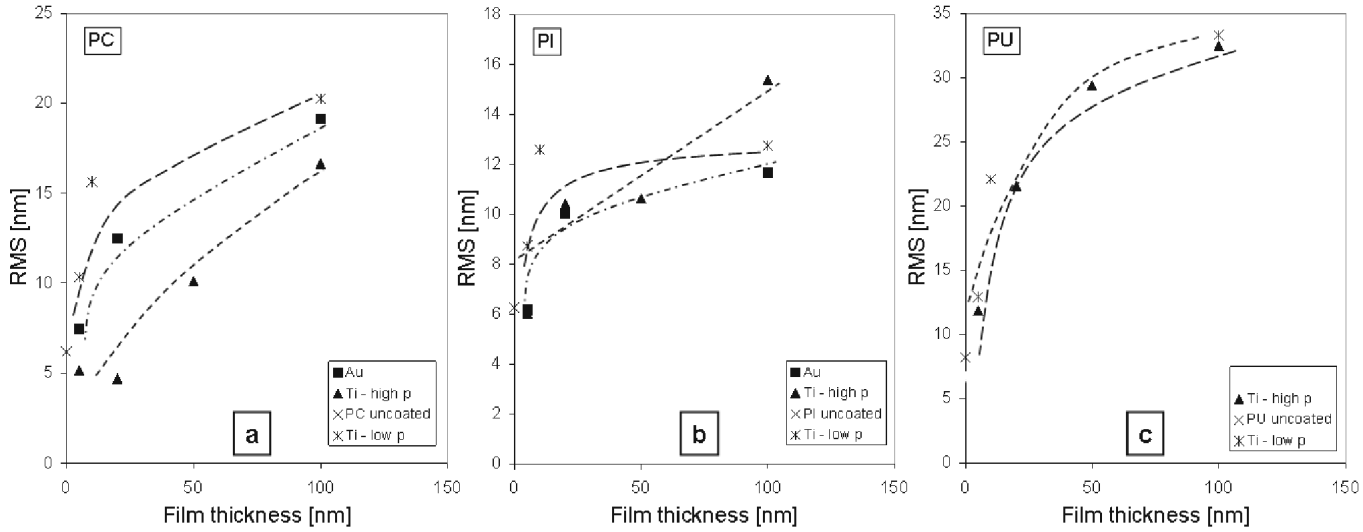

Fig. 6. Film roughness (RMS) in dependency of the film thickness for (a) PC, (b) PI, and (c) (PU) substrate materials. The applied films were deposited by PLD at different background gas pressure (Ti – low p(ressure), Ti – high p(ressure)), resulting in different energies of deposited atoms

Void formation is generally the reason of missing coalescence, causing the characteristic Zone 1 voided columnar structure [11]. Arriving atoms on a growing film cannot perch on the top of each other, but rather settle sideways into the nearest "cradle" position, in which they establish relaxed bond lengths to their nearest neighbours. This is known as "ballistic aggregation" (Fig. 5a), whereby the aggregation can result in overhang structures (Fig. 5b), which shadow the low areas from deposition ("finite-size effect"). Such mechanisms are evident at thermal deposition with a maximum of a few eV particle energy. Additional overhangs are produced by the atomic attraction of arriving vapour into the sidewalls of columns as shown in Fig. 5c. This (self-)shadowing is highly dependent on the angle of the arriving flux of particles increases towards the vapour arrival at oblique angles (Fig. 5d).

Energy-enhanced processes can reduce void formation by momentum transfer to the growing surface. Translational kinetic energy is carried by massive particles (ions and accelerated atoms) [27] (and not by electrons), as described in Subsec. 2.1. Effects of these particles are higher "impact mobility" of the adatoms, so that they can move down into the voids, and forward sputtering of other adatoms into the voids (Fig. 5e or "abstraction reaction" in Fig. 1), starting at some eV energy of the impacting particle. Impact mobility amounts to a high surface diffusion rate for a few atomic distances until the excess kinetic energy upon impact becomes dissipated into the bulk. In the forward-sputtering effect, momentum transfer from the approaching particle to the adatom causes the latter to be knocked loose and scattered forward. In practice, the structure zone Zone T is encouraged in energy-enhanced deposition by low pressures (molecular flow regime), so that incident particles neither become scattered into more oblique incident angles nor dissipate their kinetic energy in gas collisions.

Together with the smooth surface, the missing of voids in the coatings on PU reveal high enough energy for kinetic activation of surface diffusion even in magnetron sputtering with lowest vapour energy.

Focussing on the roughness dependent on the coating thickness during the initial steps of film growth, we found for most measurements a slight increase of the RMS value for 5 nm thick films compared to the uncoated substrates (Fig. 6), which corresponds to the visual impression in Fig. 3. (Some measurements show lower RMS roughness, which seems to be due to the quite high initial roughness of the used polymers.) The thickness increase to 20 nm results in a significant higher increase in RMS roughness compared to the proceeding growth afterwards (e.g. to 100 nm thick films). This behaviour is more distinct for PU ($\sim +100\%$ RMS) than for PC and PI ($\sim +60\%$ RMS).

During nucleation and early stages of film growth it's well known, that ion assistance affects the number, density

and shape of the nuclei formed at the initial stages of deposition [11]. The most commonly encountered situation at medium ion is an increase in the number of nuclei at the beginning of the deposition process (e.g. measured and calculated by [28]) due to modifications on the substrate by ion bombardment – surface defects, formed by ion impingement, become centre for nucleation of particles. Higher RMS roughness was found for all investigated 5 nm thin films too (Fig. 6), if they are deposited at higher energetic deposition ("Ti – low p") compared to the before discussed lower energetic deposition ("Ti – high p"). However, if the roughness increase is influenced by ion-bombardment induced surface modification under the proposed quenched growth conditions too, seems to be questionable: The size of the islands is even under higher energetic growth to large for Volmer-Weber type growth.

A more precise view on the coarsening of the topographic surface features – again at the lower-energetic deposition conditions ("Ti – low p") – is possible for 20 nm thick Ti films in AFM images in Fig. 7: Comparing the island-like structures (columns) found for 5 nm (Fig. 3b) to that for 20 nm thick films on PC (Fig. 7a), their height is increasing, while their lateral dimension is quite constant. Furthermore, the columns become increasingly interconnected, comparable to the features on PU. Further increasing the film thickness on PC, as shown in SEM images in Fig. 8, doesn't show such interconnections between the columns. The pulsed-DC magnetron sputtered DLC coating, deposited on ultra-smooth PC, shows all features of Zone 1 film growth according to the Thornton's structure zone model (see chapter 2.2). The amorphous columns of some tens of nanometer at the interface coarsen to amorphous cones with domed surfaces (see surface images in Fig. 8b and d). While the 300 nm thick DLC coating is covered only by a few of these larger domed tops, the 1300 nm thick coating is fully consisting of domes. The shape of the domes is well visible in the cross-section image (Fig. 8b). Additionally, voids are found due to weak binding in between the columns. Weak binding is also to reason for the crack along the column (cone) borders at the upper right. Competitive growth is, thus, an important influence in the formation of these films. However, the quite similar size of the DLC domes on the PC surface represents a type of self-assembling, nanostructured topography.

Comparing the results of topography formation on PU in even thin films to that of PC, the structural development is very different: The slightly interconnected areas at 5 nm Ti film thickness on PU (Fig. 3d) become more and more distinct in a vermicular-like surface topography at larger film thickness, e.g. shown for 20 nm thickness in Fig. 7b. This topography is fully different from the columnar on PC, although all deposition conditions were the same (same energetic conditions and same film composition). Additionally, the slopes of the vermicular-like formed hills with distinct plateau areas steepen. Figure 9 gives an impression of the topography development at increasing film thickness of PLD titanium nitride coatings: At the beginning of film growth (20 nm thick TiN, Fig. 9a) a vermicular-like structure is found on the surface (distance between parallel vermicular-like hills: ~ 4 μm), which has a nano-sized substructure (distance $\sim$100–130 nm), as shown in the highly magnified image. Even this substructure is of vermicular-like shape and has quite similar size as the topography features shown in Fig. 7b. Increasing the film thickness to 50 nm (Fig. 9b) let both topography features of the 20 nm film coarsen. Furthermore, a new superseding structure forms (distance $\sim$15 μm), which is clearly observable in the lower magnified images. The distances between

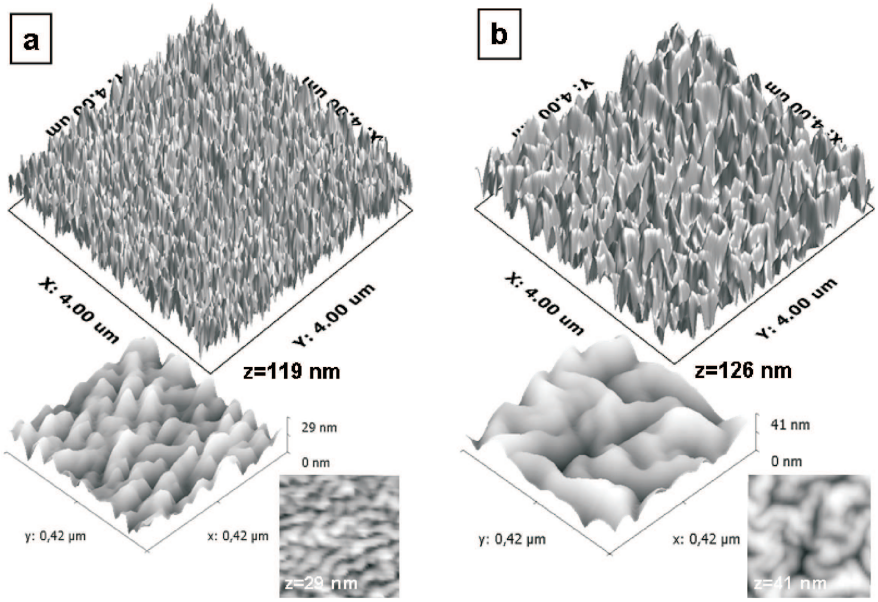

Fig. 7. AFM images of nucleation and growth structures of 20 nm thick PLD Ti coatings on PC a) and PU surfaces b), which are shown uncoated in Fig. 3a and c, respectively. The details of $\sim 400 \times 400$ nm^2 large areas show the nanostructure in two- and three-dimensional views

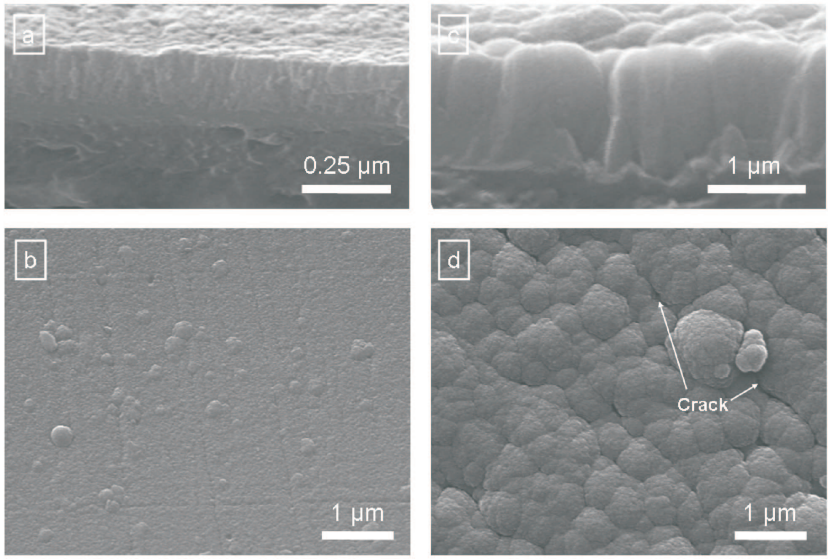

Fig. 8. SEM micrographs of the (a, c) cross-section and (b, d) surface of DC-pulsed magnetron sputtered DLC films of (a, b) 300 nm and (c, d) 1300 nm thickness on ultra-smooth PC substrates

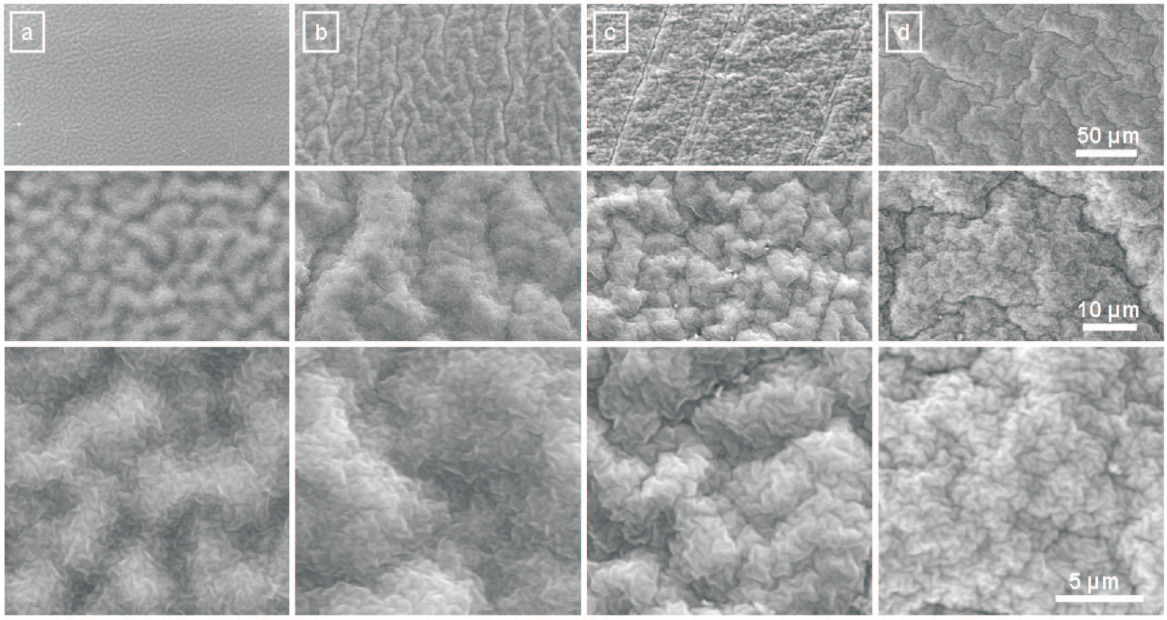

Fig. 9. SEM surface images of PLD TiN films of a) 20 nm, b) 50 nm, c) 100 nm and d) 250 nm thickness deposited on smooth PU (AFM image of uncoated substrate see Fig. 3c)

parallel parts of the vermicular hill tops of a distinct structure size are very similar on the whole images, which seems to be a general rule. In 100 nm thick TiN films (Fig. 9c) the next superseding structure (distance $\sim$60 μm) is introduced in the growth topography, slightly observable in the image taken at low magnification but better in Fig. 9d. Additionally, first hints for the formation of cracks are evident. These cracks follow the "valleys" between the vermicular-lined plateaus. Distinct crack networks can be also found in the 250 nm thick film (Fig. 9d), in which the additional vermicular surface structure, starting to be introduced in the coating growth at 100 nm thickness, forms big plateaus with the cracks in between. The cracks reach through the coating to the substrate surface, as shown in Fig. 10, along the borders of the column-like structure (Zone 1). Thus, columnar growth is found on PU too, but fully changing in its observed topography by the formation of the presented vermicular-like structure. If all the cracks in Fig. 10 are due to growth or possibly due to TEM preparation, cannot be cleared. Nevertheless, hints for cracks formed during coating are evident in the cone-shaped crystal, which started to growth after opening a crack by new nucleation. Roughness – or better – deformation of the substrate is visible by the high waviness of the surface, which is drastically larger than found for similar substrate below the 50 nm thin films in Fig. 4.

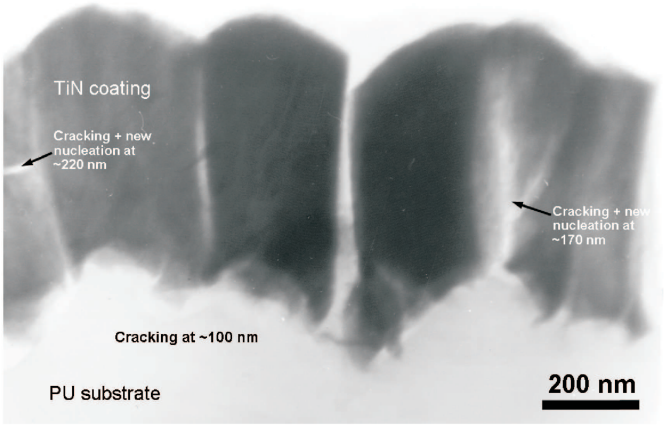

Fig. 10. TEM cross-section of a 500 nm thick PLD TiN coating on a PU substrate, showing the occurring deformation and cracking (adapted from Ref. 4)

Although first hints for crack formation are found in the 100 nm thick TiN films, three structures of differently sized, but scaled features exist even in the 50 nm thick film and must have been formed during the film growth before. What is the reason for the formation of the wave-like superseding structures with high amplitude than the film thickness? The only explanation therefore can be found in the mechanics of the film-substrate compound system, as explained later. If deformations, as mentioned above, are reason for the phenomenon, can thin films follow the surface deformation? The latter question can be easily solved due to the deformability of nanostructures, e.g. shown for 100 nm thick silicon coatings on silicon wafer substrates, which don't crack during investigation when being bended with a radius of 2 μm [15].

Additionally to the cracking, a further feature is visible for the TiN coatings of different thickness: Even in the 250 nm thick film, the smaller vermicular surface features are not lost, but coarsen and are present on the thick coating too. Thus, also the topographic structures on PU represent self-assembling nanostructures.

The coarsening mechanism of the smallest vermicular-like features was investigated by AFM. Because of the quite similar distances of the hills of each other, we calculated both RMS and lateral correlation length values as measures for the size and separation of the nanostructures. Results are presented in Fig. 11 in dependency on the coating material and the coating technique to introduce also physicochemical and vapour-energetic aspects. Interestingly, we found two regimes: Low energetic deposition (magnetron sputtering of Ti or TiN) results in a decrease of both RMS roughness and lateral correlation length at higher film thickness. This can be explained by the different formed surface topography: The surface of magnetron sputtered Ti films consists of separated, small island-like features and very large vermicular-like, wavy topographies are found on magnetron sputtered TiN. Higher energetic deposition (PLD, pulsed DC sputtering, ALS) leads to increased RMS roughness and lateral correlation length. Thus, the vermicular structures grow in their height and increase their distance at higher thickness. Higher energetic coating conditions, as found in pulsed-DC sputtering, PLD or ALS direct deposition, are, thus, decisive for forming this structure. Because the whole film is tightly bonded to the substrate (as shown e.g. [29]) and the temperature or particle energy for activation sufficient surface diffusion over some 100 atoms is missing, the separation of the vermicular hills can only be achieved by a deformation of the substrate surface or cracking. Deformation of the whole system during growth seems to the mechanism during the growth at thinner film thickness, cracking the mechanism occurring in thicker films (as visible in Fig. 9). This explains the formation of the vertically wave-like and laterally vermicular-like structures – the latter due restrictions in deformation due to the continuous film covering the whole substrate surface.

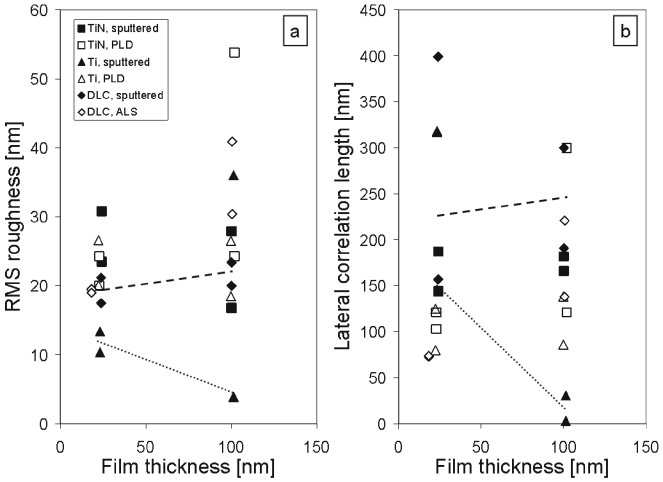

Fig. 11. a) RMS roughness and b) lateral correlation length (LCL) of different thin film materials, deposited by different deposition techniques (at different vapour energy), in dependency of their thickness on smooth PU substrates. Two values of RMS and LCL were measured independently and are given in the diagrams

The higher energetic deposition conditions are necessary in order to fill the voids between single Zone 1 columns (e.g. towards Zone T structure), which then introduces intrinsic stresses in the growing continuous film. Generally, intrinsic stresses occur on macro- and micro-level, the latter are homogenous only in the boundaries of crystals and are due to distortion at the grain boundaries or high defect densities (e.g. vacancies) [30]. In higher energetic deposition the micro intrinsic stresses result from the particle bombardment, which results additionally in implantation of atoms (both process/reactive gas and sputtered/evaporated/ablated species), straining the lattice of the substrate or growing film. Low gas pressures (molecular flow regime) lead in energetic deposition to very high compressive intrinsic stresses, higher gas pressures (towards the viscous flow regime) in moderate to low intrinsic stresses [31–33]. Additionally, intrinsic stresses are due to phase transformations, the differences in the thermal expansion coefficient, misfit at the interface, etc. The micro-intrinsic stresses generally influence the macro intrinsic stresses, which are defined to be homogenous in the whole coating. However, if the substrate is not stiff but de-

formable like polymers, local differences can be found in the stress level, as explained later. Intrinsic stress levels in the deposited films were measured by means of X-ray diffraction (XRD) or bending of a coated Si beam and are given approximately in addition to other mechanical film properties in Table 2.

For reduction of the overall strain energy in a compressive stressed coating, wrinkling has been suggested as a mode of common deformation of the substrate (surface) and the film [34]. Wrinkling is described as the formation of sinusoidal buckles on the surface, which doesn't loose their adhesion to the substrate (which distinguishes it from buckling). Thus, the main deformation mechanisms in wrinkling are bending of the substrate or of the near-surface region of the substrate (depending of the elasticity of the substrate material) together with the covering coating. This mechanism is also evident for the compressively stressed, higher energetically deposited coatings on the PU substrates.

If the in-plane stress level in the film exceeds a critical value, crack formation at the interface between the film and the substrate occurs, leading to local or global failure of the film. Hence, the nucleation and growth of individual blisters over initially de-bonded patches are found (e.g. described by [35, 36] and others). Spontaneously buckling patterns of various dimensions and structures develop, depending on the internal stresses and film thickness. Buckles occur in different topographical structures, such as typical circular blisters (hemispherical caps), worm-like structures or straight-sided wrinkles. The different shapes of buckles might be correlated with the elastic and bending energy stored in the lifted area of the film [37]. However, the topography of buckled coatings on polymers is drastically different from the observed surfaces for the coated PU, shown in Fig. 9 (see e.g. for buckled coating surfaces on polymers [4]).

Both phenomena were illustratively shown by Mylvaganam et al. [38] in structural calculation – releasing biaxial compressive stresses of the film to the substrate – on the atomic scale (Fig. 12). These calculations, based on forces between the atoms, show for thin diamond coatings on (100) orientated single-crystal silicon substrates [38] two distinct characteristics: (1) The formation of a clustered surface topography with a quite regular arrangement of the wrinkles (buckles) (Fig. 12b) allows a relaxation of the compressive stress in the coating by its deformation. The "volume" of the coating is increasing, clearing space for the expansion of the grown lattice. But full stress relaxation is only possible in some regions – the formation of the wavy surface creates in the curved areas again tensile and compressive stresses – using the example of the top of such a wave, the upper part of the coating is tensile stressed, the lower part compressive stresses (and vice versa for a valley of such a wave) [34] (non homogenous macro-intrinsic stress). Consequences of this behaviour are shown in the following. (2) The formation of a disordered surface region of the silicon (Fig. 12a) is found due to the growth stresses developing in the coating. Loosing the crystal structure in the near-surface region of the substrate results in lower packing density of the atoms and, hence, in a worse bond allowing easier deformability by higher elasticity and lower stress levels for plastic flow mechanisms (weak-boundary layer). In Fig. 12a the partly delamination of the coating in the near-surface region of the substrate was found (exceeding the fracture stress of the interface).

Table 2
Mechanical properties and intrinsic stresses in magnetron sputtered, PLD and ALS grown coatings [15, 32, 33]

	Elastic modulus [GPa]	Hardness [GPa]	Intrinsic stresses/ measurement method		
			Compressive stress [GPa]	Thickness [μm]	Substrate material
Titanium/sputtered	110	3	~0.2/XRD	1 μm	Si
Titanium/PLD	120	5	~0.65/XRD	1.5 μm	Austenitic steel
Titanium nitride/sputtered	250	15	~0.5/XRD	1 μm	Si
Titanium nitride/PLD	290	25	6–10/XRD	1 μm	Austenitic steel
DLC/sputtered	160	16	~0.5–1/bending beam	1 μm	Si
DLC/ALS	160	25	~1–2/bending beam	600 nm	Si

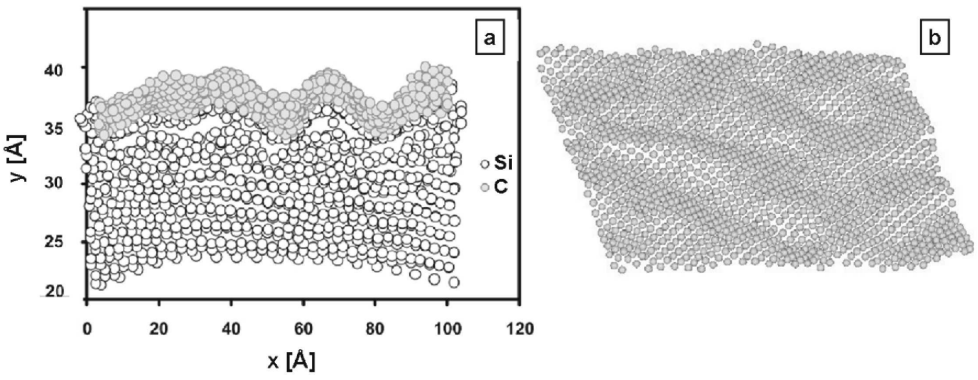

Fig. 12. a) Cross-section of portion of the film and substrate and b) topography of the film after releasing the biaxial stresses (after Ref. 35)

These theoretical considerations of the effects of growth stresses on the coatings performance reveal, that mainly the mechanical properties of the substrate, coating and the interfacial region control the deformation. Thus, it's clear, while different topography is formed on "soft" PU and "stiff" PI or PC substrates: PC possesses (according to Table 1) a quite low elongation at fracture and an elastic modulus comparable to most thermoplastic polymers. It's thermal resistance is quite high and, thus, the viscoelastic tendency to mechanical softening (decrease of elastic modulus and increase of elongation at fracture) is low.

However, the quite "stiff" material properties are not able to prevent deformation of the substrate surface at the beginning of the thin film formation: The island-like structure (or better: the wrinkles) in Fig. 3b is a caused by the intrinsic stress in just a 5 nm thick continuous film, homogenously covering the substrate surface. Further growth does not introduce further distinct wrinkles of larger size as found for PU but leads to growth of regular Zone 1 columns (Fig. 7a) with distinct voids at the boundaries. Further intrinsic growth stresses result in very large waves (wrinkles) with tens of μm hill-to-hill distance. The origin of the cracks found in the SEM surface images (Fig. 8d) may be due to the described intrinsic stress caused deformation with large wrinkles or by swelling. Swelling stresses could occur, but are very unlikely due to the low water absorption of 0.35% at the saturation point even if the water content of the polymer after the vacuum coating treatment was minimized.

PI is stiffer, but more brittle than PC (4–8% elongation at fracture). Thus, the quite similar behaviour to PC in the first stage of film nucleation and some 20 nm thick film growth can be easily explained. However, at higher thickness (500 nm PLD Ti, as shown in Fig. 13) vermicular-like structures form to reduce the intrinsic growth stress by the higher energetic PLD film growth compared to the lower-energetic DLC film growth on PC.

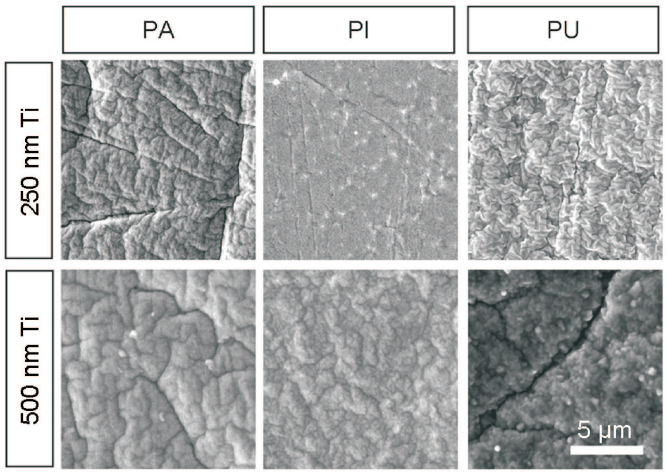

Fig. 13. SEM surface images of 250 and 500 nm Ti films on PA, PI and PU substrates

For PU as the investigated material of highest compliance (lowest elastic modulus and longest elongation at fracture) wrinkling is the dominant factor in thin film topography formation. Even in very thin coatings (5 nm), the structure of interconnected "islands" (Fig. 3d) is caused by intrinsic growth stresses. Stress relaxation is afterwards a continuous process, in which wrinkles form, if the substrate surface isn't able to support "load support" for the increasing stress, building up in the growing coating (Fig. 9). The increase in the film thickness reduces cumulatively the flexibility (deformability) of the coating, but increases the compressive growth stress. Thus, mechanisms for intrinsic stress relaxation change first to the formation of larger wrinkles (also due to the higher "load support" by the now coated compound) and later to cracking. Accordingly, the small wrinkles are covered with subsequently deposited layers, become stiffer and slightly coarsen – as shown for the 20 nm thick coating in Fig. 9a. However, the intrinsic stress can be reduced by forming larger wrinkles as a superseding structure. The high elasticity of PU can follow this deformation and the even the next, when the next superseding wave-like superseding structure is formed, as shown for the 50 nm thick films (Fig. 9b). However, the thicker the film the lower it's deformability and reducing the stress by forming a further superseding structure (Fig. 9c,d) leads to cracking of the film and a crack network covering the whole surface (Fig. 9d and 13).

Such crack networks are evident for the 500 nm thick TiN coating (Fig. 10): The first crack network cut the about 100 nm thick film in parts of 250 nm length, as found close to the interface. These parts are separated 100 nm from each other in the TEM image, but not as far just after cracking. This can be concluded from the cone-like growth shape of the TiN columns, seeding on these parts. Thus, the vermicular-shaped topography of the wrinkles – at least for thicker films $>$100 nm (as shown in Fig. 10) – is not formed only caused by elastic and plastic deformation of the compound system coating-polymer (surface), but also by cracking. Further cracking occurred in the investigated areas of this TEM image at about 170 nm and 220 nm film thicknesses as visible by the new cone forming on the right and very left side, respectively. Growth of new cone-shaped, but one-directional elongated columns seems to be one origin for coarsening of the vermicular structures. Thus, the introduction of superseding structures results in cracking through the coating along weak spots (voids) of the old topography. Although this is rather not observable by microscopic methods, we predict, that even for $\sim$10 nm thick films during the introduction of a superseding structure (e.g. 20 nm films in Fig. 9a) the mechanism of cracking occurs. FEM simulations of deformation and cracking in thin film formation on soft substrates support this theory [4].

Although PA is much stiffer than PU due to its quite high elastic modulus in the first part of deformation, the high elongation at fracture of $\sim$170% allows high plastic deformation after reaching the yield strength of $\sim$65 MPa. Reasonably, the topography formation on PA (Fig. 13) is quite clear: The high elongation to fracture allows the wrinkle formation of the coatings, however, the wrinkle structure is much coarser than found for PU due to the higher yield strength.

Table 3
Separation of the parallel tops of the smallest wrinkle structures on PU for different coatings and deposition techniques

Coating		Average wrinkle separation [nm]	
Material	Deposition technique	20 nm thick film	100 nm thick film
Ti	DC sputtering	No wrinkle formation	
	PLD	120	160
TiN	DC sputtering	300	500
	PLD	140	170
DLC	DC pulsed sputtering	110	160
	ALS (PACVD)	160	160

As discussed above, the wrinkling phenomenon requires high enough intrinsic growth stresses in the coatings. Discussing now the distinct influence of the vapour energy during deposition on wrinkling, a comparison of the distance of the smallest wrinkle structures (starting their formation at ∼5–10 nm thickness) is of high interest (Table 3). The threshold in compressive stress seems to be around 0.5 GPa. No wrinkles are formed on sputtered Ti films due to the too low intrinsic stress in low-energetic, sputtered deposition. On sputtered TiN films we found extremely large parallel wrinkles of about 300 to 500 nm distance and no hints for smaller wrinkles. Compared to the sputtered Ti films, the energy of the deposited particles was quite similar, but the formation of the stoichiometric TiN composition both stiffens the compound (higher elastic modulus) and, thus, introduces intrinsic grow stresses (0.65 GPa). However, they are too low to form the smaller wrinkling structure (∼120 nm), found for all other coatings. Higher growth stress, as found in higher energetic PLD TiN, decreases the wrinkle separation. Although the growth stress for PLD Ti is smaller than for PLD TiN, the wrinkles are closer to another, which is due to the lower elastic modulus of Ti. The same can be stated for the lower-energetically DC sputtered DLC film in comparison to PLD TiN. For the ALS DLC, the higher hardness (due to the lower H content) is the reason for the increase compared to sputtered DLC.

This result confirms, that the wrinkle formation is a function of substrate as well as coating material and its mechanical properties, the thickness of the coating and the particle energy during deposition influencing the intrinsic growth stresses.

5. Conclusions

The current work showed the growth phenomena in vacuum deposition of inorganic coatings on polymer substrates. Compared to other substrate materials like steels or ceramics, the microstructure and topography formation is highly dependent not only on the coating material, its thickness and the energy of the deposited particles, but also on the mechanical properties of the substrate material. Generally, the growth of the coatings follows the well known structure zone models – however, thermal activation of surface diffusion is impossible in most cases due to the temperature restrictions of polymers (softening, melting). Thus, only Zone 1 and T structures will be developed, dependent on the energetic conditions (deposition technique and process gas pressure). The higher the energy of the deposited particles, the higher is the trend towards Zone 1, but the higher are the intrinsic compressive growth stresses. While stiff polymers can withstand a deformation of the surface-near region under highly stressed and dense thin films, softer and more flexible polymers start to form wrinkles, if the adhesion (chemical binding) of the coating on the substrate is strong enough. Wrinkles are a phenomenon of stress relaxation of the whole compound system and occur in several superseding structures when increasing the film thickness. If the coating cannot follow the deformation of the substrate surface by elastic or plastic deformation, crack are formed in the coating – starting even in some 10 nm thick films on highly deformable polymers.

While coatings stiff substrates develop a dome-shaped topography, depositing on soft substrates results in vermicular-like structures. However, all these topographies are perfect examples of fully-reproducable self-assembling nanostructures.

Acknowledgements. Financial support of this work by the Austrian Federal Ministry of Traffic, Innovation and Technology, the Austrian Industrial Research Promotion Fund (FFG) within the frame of the Austrian Nanoinitiative and the MNT-ERA-NET program, the Government of Styria, and the European Union in the frame of the EFRE is highly acknowledged. Specials thanks for discussion and contributions to the work are dedicated to Mag. Markus Kahn (Laser Center Leoben), Dr. Thomas Schöberl (Erich-Schmid Institute, Austrian Academy of Sciences), Oliver Miskovic (Institute of Physics, University of Leoben) and Roman Major (IMIM-PAN Krakow).

REFERENCES

[1] B. Rother and J. Vetter, *Plasmabeschichtungsverfahren und Hartstoffschichten*, Dt. Verlag für Grundstoffindustrie, Leipzig, 1992.

[2] S.M. Metev and V.P. Veiko, *Laser-assisted Microtechnology*, Springer, Berlin, 1998.

[3] A.D. Akhsakhalyan, B.A. Biryutin, S.V. Gaponov, A.A. Gudkov, and V.I. Luchin, "Processes occurring in an erosion plasma during laser vacuum deposition of films – 1. Properties of a laser erosion plasma in the inertial-expansion stage", *Soviet Physics. Technical Physics* 27, 969–973 (1982).

[4] J.M. Lackner, "Industrially-scaled hybrid pulsed laser deposition at room temperature", *Habilitation Thesis*, Polish Academy of Sciences – Institute of Metallurgy and Materials Science, Cracow, 2005.

[5] J.A. Thornton, "Influence of apparatus geometry and deposition conditions of the structure and topography of thick sputtered coatings", *J. Vacuum Science and Technology* 11, 666–670 (1974).

[6] R. Messier, A.P. Giri, and R.A. Roy, "Revised structure zone model for thin film physical structure", *J. Vacuum Science and Technology* A 2, 500–503 (1984).

[7] L. Hanley and S.B. Sinnott, "The growth and modification of materials via ion–surface processing" *Surface Science* 500, 500–522 (2002).

[8] J.F. Ziegler, J.P. Biersack, and U. Littmark, *The Stopping and Range of Ions in Solids*, Pergamon Press, New York, 1985.

[9] D.C. Jacobs, "The role of internal energy and approach geometry in molecule/surface reactive scattering", *J. Physics: Condensed Matter* 7, 1023–1045 (1995).

[10] K. Seshan, *Handbook of Thin Film Deposition – Processes and Technologies*, Noyes Publications/ William Andrew Publishing, Norwich, 2002.

[11] D.L. Smith, *Thin Film Deposition: Principles and Practice*, McGraw-Hill, New York, 1995.

[12] B.A. Movchan and A.V. Demchisin, "Structure and properties of thick vacuum-condensates of nickel, titanium, tungsten, aluminum oxide, and zirconium dioxide", *Physics of Metals and Metallography* 28, 83–85 (1969).

[13] J.A. Thornton, "High rate thick film growth", *Annual Review of Materials Science* 7, 239–260 (1977).

[14] M. Ohring, *Materials Science of Thin Films: Deposition and Structure*, Academic Press, New York, 2002.

[15] J.M. Lackner, "Innovative coating by pulsed laser deposition", *PhD Thesis*, University of Leoben, Leoben, 2003.

[16] M. Kahn, *PhD thesis*, Montanuniversität Leoben, Leoben, 2010, to be published.

[17] H. Sächtling, *Kunststoff-Handbuch*, Hanser, München, 1992.

[18] *TrueGage*, TrueMap v4.0, 2009.

[19] *Nanotec*, WSxM v3.0, 2009.

[20] D. Nečas and P. Klapetek, *AFM and SPM software, Version 2.17*, 2009.

[21] J.C. Teichert, "Self-organization of nanostructure in semiconductor heteroepitaxy", *Physics Report* 365, 335–342 (2002).

[22] S.K. Sinha, E.B. Sirota, and S. Garoff, "X ray and neutron scattering from rough surfaces", *Phys. Rev.* B 38 (4), 2297–2311 (1988).

[23] Ch. Teichert, A. Haas, G.M. Wallner, and R.W. Lang, "Nanometer scale of characterization of polymer films by atomic-force microscopy", *Macromolecular Symposia* 181, 457–466 (2002).

[24] H. Jehn, *Hartstoffschichten zur Verschleißminderung,* Deutsche Gesellschaft für Metallkunde, Oberursel, 1987.

[25] W. Ensinger, "Low energy ion assist during deposition – an effective tool for controlling thin film microstructure", *Nuclear Instruments and Methods in Physics Research* B 127/128, 796–808 (1997).

[26] J.M. Lackner, W. Waldhauser, and T. Schöberl, "Film growth phenomena in high-energetic room temperature pulsed laser deposition on polymer surfaces", *Surface and Coatings Technology* 201, 4037–4039 (2006).

[27] K.H. Müller, "Summary abstract: molecular dynamics studies of thin-film deposition", *J. Vacuum Science and Technology* A6, 1690–1961 (1988).

[28] H.A. Durand, K. Sekine, K. Etoh, K. Ito, and I. Kataoka, "Relation of initial thin film formation to defects induced by low energy ions", *Thin Solid Films* 336, 42–48 (1998).

[29] R. Major, J. Bonarski, J. Mogiel, B. Major, E. Czarnowska, R. Kustosz, J. M. Lackner, and W. Waldhauser, "Elastic TiN coating deposited on polyurethane by pulsed laser", *Surface and Coatings Technology* 200, 6340–6345 (2006).

[30] D.S. Rickerby, A.M. Jones, and B.A. Bellamy, "X-ray diffraction studies of physically vapour-deposited coatings", *Surface and Coatings Technology* 37, 111–137 (1989).

[31] D.S. Rickerby, G. Eckold, K.T. Scott, and I.M. Buckley-Golder, "The interrelationship between internal stress, processing parameters and microstructure of physically vapour deposited and thermally sprayed coatings", *Thin Solid Films* 154, 125–141 (1987).

[32] J.M. Lackner, W. Waldhauser, R. Ebner, B. Major, and T. Schöberl, "Structural, mechanical and tribological investigations of pulsed laser deposited titanium nitride coatings", *Thin Solid Films* 453–454, 195–202 (2004).

[33] J.M. Lackner, W. Waldhauser, R. Berghauser, R. Ebner, B. Major, and A. Fian, G. Jakopic, „New trends in coating: Room temperature deposition of titanium-based films", *Materials Engineering* 140, 611–615 (2004), (in Polish).

[34] X.-Y. Gong and D.R. Clarke, "On the measurement of strain in coatings formed on a wrinkled elastic substrate", *Oxidation Metals* 50, 355–376 (1998).

[35] A. Kinbara, S. Baba, N. Matuda, and K. Takamisawa, "Mechanical properties of and cracks and wrinkles in vacuum-deposited MgF2, carbon and baron coatings", *Thin Solid Films* 84, 205–212 (1981).

[36] N. Matuda, S. Baba, and A. Kinbara, "Internal stress, young's modulus and adhesion energy of carbon films on glass substrates", *Thin Solid Films* 81, 301–305 (1981).

[37] A. Pundt, E. Nikitin, P. Pekarski, and R. Kirchheim, "Adhesion energy between metal films and polymers obtained by studying buckling induced by hydrogen", *Acta Materialia* 52, 1579–1587 (2004).

[38] K. Mylvaganam and L.C. Zhang, "Residual stress induced atomic scale buckling of diamond carbon coatings on silicon substrate", *Thin Solid Films* 425, 145–149 (2003).